

TOWARDS AERODYNAMIC DESIGN BY OPTIMISATION OF TRANSONIC TRANSPORT AIRCRAFT IN A MULTI-DISCIPLINARY CONTEXT

G. Carrier, S. Mouton, M. Marcelet, C. Blondeau

ONERA

29, avenue de la Division Leclerc BP 72

92322 Châtillon

France

ABSTRACT

Through the presentation of three recent and ongoing research works, this paper illustrates different approaches to shape optimisation of aircraft components requiring both aerodynamic and structural disciplines to be taken into account. Pragmatic solutions that allow applying aerodynamic optimisation techniques and tools into a multi-disciplinary context have been chosen. Actual applications of “aerodynamic-centric” multi-disciplinary optimisations of two aero-structural systems presenting weak coupling between the two disciplines are described. An extension of the aerodynamic adjoint-based optimisation technique enabling the optimisation of aero-elastic systems with strong coupling is also introduced.

1. INTRODUCTION

The progresses achieved in the field of aerodynamic shape optimisation over the last two decades have permitted a progressive dissemination of “design by optimisation” approach and its associated technologies in the aerodynamics design offices of aircraft makers. Indeed, thanks to continuous improvements of Computational Fluid Dynamics codes [1], geometry manipulation tools [2][3], computational grid generation and deformation techniques, and also numerical optimisation algorithms, the robustness and performance reached by these different necessary components of an optimisation process provide today sufficient maturity and flexibility to start being used in industry for the aerodynamic design work [4]. An important step has also been accomplished with the introduction of sensitivity calculation by the adjoint techniques [5][6] which significantly increased the possibilities offered by aerodynamic optimisation techniques [7][8][9].

Today, a new frontier for design optimisation is to account for the complex multi-disciplinary environment inherent to the design process of aerospace products. Multi-Disciplinary Optimisation (MDO) has become a very active field of research and is intended to provide new techniques and tools to improve the design process of complex multi-disciplinary systems, i.e. taking into account the complexity of the different interacting disciplines that impact the overall performance of the system. Successful applications of MDO have demonstrated its usefulness for system design in conceptual and preliminary design stages. However, the application of MDO for detailed design, which requires the use of high-fidelity experts methods in the different

disciplines is not yet mature enough [10] to be used in an industrial context.

A pragmatic approach towards high-fidelity MDO is presented in this paper from the standpoint of the aerodynamicist. Accounting for the impacts of the geometry modifications on the other disciplines during the aerodynamic design optimisation of an aircraft may be required. The design of many aircraft components provides examples of such situation where the impact on the aircraft structure has to be considered.

Recent and ongoing research activities conducted at ONERA on this topic are illustrated in this paper with three different approaches of aerodynamic-centric aero-structural optimisations accounting for the structure discipline. The two first sections illustrate applications of aerodynamic optimisation of aircraft components where simple reduced models are used to evaluate the impact of the design geometry modifications on the structure. These approaches are applicable to system with weak coupling or decoupled disciplines analysis. The last section presents the current status of the development of a high-fidelity adjoint sensitivity analysis technique applicable to system with strong coupling between aerodynamics and structure.

2. OPTIMISATION OF THE ENGINE PYLON OF A TRANSPORT AIRCRAFT

This first application of MDO deals with the aerodynamic and structural optimisation of the powerplant integration under the wing of a transonic transport aircraft. Indeed, the larger size of modern aircraft engines with high by-pass ratio leads to increasing difficulties regarding engine integration under the wing [11] [12]:

- on the aerodynamic side the features of the transonic flow on the whole wing are modified by the propulsion system, causing drag penalties;
- on the structure side the large forces to sustain lead to heavy mechanical parts.

From experience, the consequences of drag and mass penalties on the aircraft operating costs are of the same order of magnitude. It advocates for an MDO approach so that properly accounts for both penalties and compromise between them. In this work, carried out within the European project *VIVACE*, the loosely coupled character of the problem allows us to use a hierarchical optimisation approach.

2.1. Objective & strategy

The objective function selected as a first order approximation of aircraft operating costs is a linear combination of the drag increment at cruise conditions J_{aero} and the mass increment of the primary structure of one pylon J_{struct} . It writes as: $J = J_{aero} + 4 \cdot J_{struct} / k$ where J is expressed in terms of drag units, k is an exchange rate between mass and drag and the factor 4 is the number of engines and hence of pylons.

The principle of the multi-disciplinary optimisation performed in this engine pylon design work formalises a well-known hierarchical procedure. It relies on the identification of parameters having a coupling role between disciplines. Those are addressed at the higher level. Other parameters are discipline specific and are addressed at the lower level. This lower level then consists in as many uncoupled optimisation problems as involved disciplines. They can be addressed independently, raising information on demand to the upper level. Moreover, during the design process, the behaviour of the low-level disciplines is modelled by surrogate models. For each discipline, the surrogate model is built thanks to the procedure described FIG 1. A set of n individuals (each of whom is called a *configuration* in the following) is defined by sampling in the high-level design space. Each of these configurations is examined at the lower level, that is to say an optimisation is performed on the low-level objective by varying low-level parameters. Therefore, the best performance of each configuration sampled is derived. A Kriging method [13] is then used to interpolate the data in the whole high-level design space. This procedure was applied independently for structure and for aerodynamics, with independent samples.

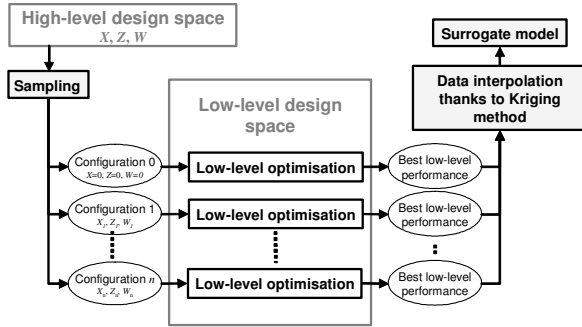


FIG 1. Building of surrogate model

The pylon optimisation reported in this section is a two-level, two-discipline problem. The higher level comprises three parameters which are known to impact both weight and drag. (see FIG 2):

- X is the variation of longitudinal position of the engine;
- Z is the variation of vertical position of the engine;
- W is the variation of pylon width.

Variation means difference with respect to a baseline shape, and in the following, these parameters are presented adimensioned by the wing local chord C .

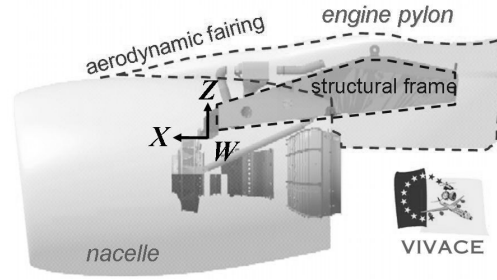


FIG 2. General arrangement of powerplant and high-level design variables

The lower level deals on the one hand with detailed sizing of the pylon structure, and on the other hand with the shape of the aerodynamic fairings. The detailed sizing of the pylon structure does not modify the external shape of the pylon and therefore has no influence on the aerodynamic performance. Reciprocally, the shape of the fairings around the pylon does not modify its primary structure if enough inner room is preserved.

2.2. Structure optimisations & response surface

The optimisations of the pylon structure were performed at AIRBUS France and are reported here for the sake of coherency but with only few details. The structure objective function J_{struct} is the increment of mass of the primary structure of one engine pylon. The constraints are the maximum stress values in the panels and spars as well as some manufacturing constraints. Several loads cases are considered, including limit loads and fatigue cases. For each of the 10 sampled high-level configurations, a finite-element model is automatically built. The 27 lower-level design variables are thicknesses of the pylon spars and panels in several areas. A gradient algorithm using finite difference gradient was used, starting from arbitrary thicknesses. Mass is determined from simple geometrical computations, and the stresses for each load case are computed by solving the static linear equation.

The response surface derived thanks to Kriging method is presented in FIG 3, where mass increments are adimensioned by the mass of the baseline pylon M_0 .

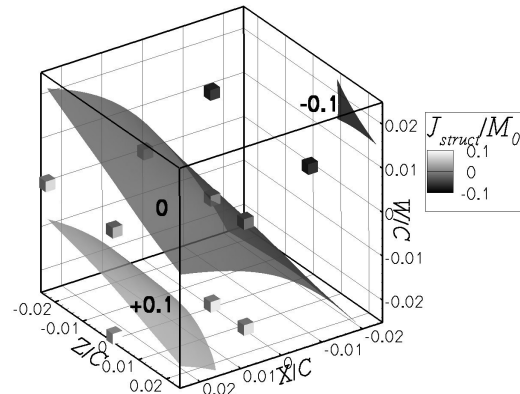


FIG 3. Optimised structure response surface displaying iso-surfaces of mass increments

The tendencies and values observed are in agreement with experience, i.e. the pylon gets heavier when:

- its length is increased ($X>0$);
- its height is increased ($Z<0$);
- its width is decreased ($W<0$).

The first two points arise from geometrical considerations and from the increased lever arm of the fan-blade-off forces. The last point is related to the reduced moment of inertia of a thinner frame which forces the designer to thicken its components to sustain the same forces.

2.3. Aerodynamic optimisations & response surface

The surrogate model for aerodynamics is built thanks to the optimisation of 9 sampled configurations in the high-level design space. They were chosen in the same parameter range as the one used to build the structure surrogate model i.e. $\pm 0.024.C$. For each configuration, an initial external shape of the pylon is built by the CAD tool. The shape is then improved thanks to the optimisation process described in this section.

2.3.1. Objective, constraints & parameterisation

The objective of the shape optimisation is to minimize drag at fixed lift. Considering the small lift variations, the drag at iso-lift is extrapolated from the drag at iso-AoA. Changes in friction drag are also negligible. The aerodynamic objective function then writes as:

$$J_{aero}(\alpha) = C_{Dp}(\alpha) - \left(\frac{dC_{Dp}}{dC_{Lp}} \right)_{\alpha=0} (C_{Lp}(\alpha) - C_{Lp}(\alpha=0)),$$

where α is the vector of low-level design variables. The first order extrapolation of drag translates into a penalty term in the objective, the penalty coefficient being the local slope of the polar curve. No constraint is imposed during the optimisation. Design variables are bounded both to maintain minimum pylon width and to ensure that the quality of the mesh remains sufficient to be computed. The gradient algorithm used for aerodynamic optimisations is the BFGS quasi-Newton algorithm.

The parameterisation chosen attempts to take into account available information [11][12][14][15][16] and in-house experience [17][18][19]. It comprises 19 parameters controlling the position and height of 17 Hicks-Henne bumps [20] spread on the pylon surface. The shape of the wing remains unchanged.

2.3.2. Flow & gradient computations

The aircraft is examined at cruise conditions, with an upstream Mach number of 0.85 and a Reynolds number of 20 millions. The flow in each engine is simulated thanks to appropriate boundary conditions on the entry and exit planes. Complex transonic flow and a large contribution expected from viscous pressure drag advocate for a Reynolds-Averaged Navier-Stokes physical modelling [21]. However, to curb the large computational time implied, the boundary layer is modelled only on the wing and on the outboard pylon. Final mesh size reaches around 1.5 millions nodes and it remains coarse considering the complexity of the geometry, so that results

have to be considered with caution. The *elsA* software [1] is used to perform the computations, using a Roe upwind scheme with a Harten entropic correction. It is extended to second order accuracy with MUSCL method using van Albada limiter. Implicit LU-SSOR method and backward Euler scheme are used during the resolution. A two-level multigrid method is also used and a converged solution is obtained in 500 cycles, with L_2 -averaged residuals loosing about 2.5 orders of magnitude and forces coefficients well stabilised.

The selected method of optimisation requires the knowledge of the gradient of the objective function J_{aero} with respect to each design variable. Assessment of this gradient by finite difference method would have implied to run a number of computations proportional to the number of design parameters, which would have been unaffordable. Instead, an alternative method based on the adjoint state and developed in the last decade [6][5] was used. This method was added to the *elsA* software [22][7] and used with success at ONERA [8][9] and AIRBUS France [4] [21] on inviscid and viscous flow cases. Some additional validations were carried out for this large 3D RANS case [25].

2.3.3. Optimised aerodynamic response surface

After optimising the shape of each sample, the aerodynamic response surface is derived yielding results presented in FIG 4.

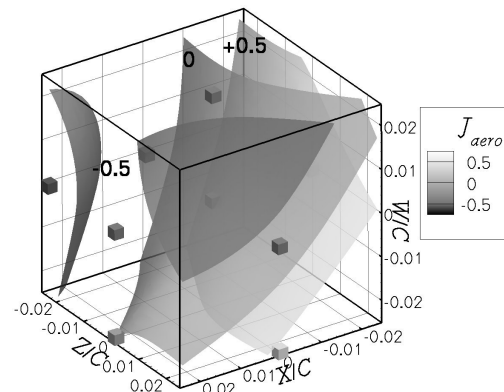


FIG 4. Optimised aerodynamic response surface displaying iso-surfaces of drag increment (in d.c.)

The drag mainly tends to be lowered:

- with engine longitudinally farther from the wing ($X>0$);
- with wider pylon ($W>0$).

As it has already been observed in [12] and [19], the sensitivity of drag with respect to the Z variable is low. The optimum is predicted at $X/C=0.011$, $Z/C=0.024$, $W/C=0.024$.

2.4. Global response surface and optimum

Gathering information from the structure and aerodynamic surrogate models thanks to the exchange rate k allows us to derive the response surface for the multi-disciplinary

problem displayed in FIG 5. At this stage, it is easy to vary k and to observe its effect on the final result, for example to derive a Pareto front.

Considering the limited number of high-level parameters and the negligible computation time of the surrogate model, the optimum is easily and rapidly found by any algorithm or even by systematic exploration of the design space, such as used to plot the FIG 5. The multi-disciplinary optimum is predicted at $X/C=0.011$, $Z/C=0.024$, $W/C=0.024$. At this point, a gain on J of -1.37 d.c. compared to the baseline configuration is predicted. In the present case, the problem is mainly driven by aerodynamic. Moreover, both disciplines exhibit negative sensitivities with respect to W and Z , which prevents a compromise to be found in the searched area of the design space and thus causes the optimum to be located on the border, in a region of large Kriging standard error. Enriching the aerodynamic sample in this region would permit to increase the accuracy of the solution found.

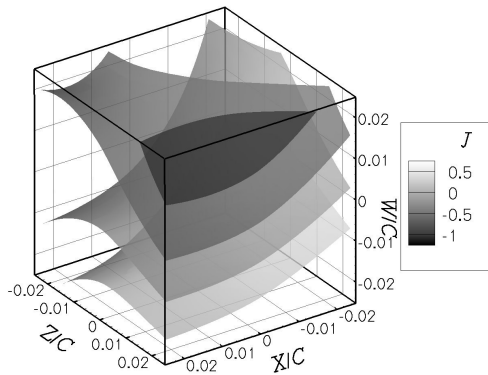


FIG 5. Multi-disciplinary optimised response surface displaying iso-surface of J (in d.c.)

2.5. Conclusions & perspectives

The hierarchical strategy used during this work does not require exchange of information between each discipline during the lower level optimisations, enabling an autonomous work in each discipline and the independent use of high fidelity tools, which is certainly an advantage considering usual organisation of industrial companies. However, it is limited to applications where the different disciplines are coupled through a limited number of parameters to enable the construction of consistent surrogate models with an acceptable number of samples. For such cases, a valuable knowledge of the whole design space may be derived, and the trade-off between disciplines can be chosen *a posteriori*. The final optimisation can be performed very easily from these surrogate models. The aerodynamic optimisations rely on the adjoint method, demonstrating it is now mature enough to be applied to complex 3D turbulent cases encountered in industrial design. The Kriging method showed promising results even though full benefit was not taken from this surrogate technique. For future use of this method, it is recommended to build a first response surface with few samples, and then refine it by adding sample points at locations of low confidence and probable minimum. This requires a flexible and short-time response

tool to sample an additional point and would benefit from an automated process.

3. AERO-STRUCTURAL OPTIMISATION OF A TRANSPORT AIRCRAFT WINGLET

The second application of multi-disciplinary optimisation presented in this section focuses on the design of an integrated winglet for a civil transport aircraft.

3.1. Description of the winglet design problem

The design of such a wing-tip device is mainly driven by two disciplines, aerodynamics and structures. For a fixed wing span, the introduction of an integrated winglet offers cruise performance improvements thanks to a lift-induced drag reduction. These performance improvements are obtained at the price of an increased structural weight of the wing due to the wing box reinforcement necessary to carry the additional aerodynamic wing bending moment introduced with the winglet and to the winglet weight itself.

3.2. Baseline configuration

The reference configuration used for this winglet design work corresponds to a generic transport aircraft wing-body configuration (FIG 6). It includes a large integrated winglet

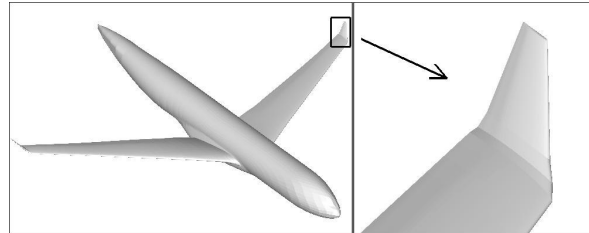


FIG 6. Baseline aircraft configuration for the winglet design study

3.3. Approach to solve the winglet multi-disciplinary problem

A simplified multi-disciplinary problem of the “real world” winglet design has been considered in this work. First, for the reasons mentioned previously, only the two disciplines aerodynamics and structure have been considered (aero-structural multi-disciplinary problem). In addition, several assumptions have been made to limit the width of the exchanges between aerodynamics and structure disciplines in order to provide maximum autonomy between these two disciplines. These additional simplifying hypotheses are:

- a rigid wing assumption during aerodynamic analyses;
- a simplified aerodynamic-structure coupling (though the wing root bending moment only).

3.3.1. Geometry design parameters

Three design parameters have been used to define the winglet geometry, respectively the winglet height, its leading-edge sweep angle and its tip aerodynamic twist,

as presented in FIG 7.

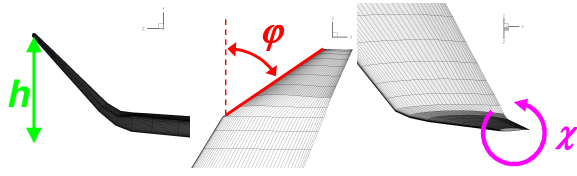


FIG 7. Design parameters of the winglet geometry: winglet height, leading-edge sweep and winglet tip twist.

3.3.2. Optimisation problem formulation

The optimisation problem has been formulated, similarly to the previous engine pylon optimisation, as a minimisation problem of an aero-structure composite objective function defined as:

$$J(\alpha) = CD_{cruise}(\alpha) + \frac{\Delta Weight_{wing}(\alpha)}{k}, \text{ with } \alpha \text{ being the}$$

winglet geometry variable, CD_{cruise} the aerodynamic drag coefficient in cruise flight condition, $\Delta Weight$ the variation of the structural weight of the complete wing structure (with respect to the baseline configuration) including the main wing box and the winglet structure and k a trade-off coefficient weighting the relative influence of disciplines. The value of this k coefficient has been fixed to roughly 400 kg per drag count in these optimisations (an arbitrary small value to better equilibrate the influence of both disciplines).

The minimization of the function is performed under a set of constraints (either explicit or implicit):

- minimum lift in cruise condition ($CL_{cruise} \geq 0.5$);
- wing box structure sized to sustain the critical 2.5g manoeuvre load case.

3.3.3. Design conditions

Two flight conditions were evaluated for each winglet designs with aerodynamic CFD calculations:

1. The investigated cruise condition corresponds to Mach 0.82, $CL=0.5$ for a Reynolds number of 50 millions; A far-field drag extraction technique [26][27] was used to evaluate accurately the cruise performance CD_{cruise} from the corresponding CFD flow solution obtained with the *elsA* code;
2. A 2.5 g longitudinal manoeuvre conditions corresponding to Mach 0.6, $CL=0.7$ and a Reynolds number of 70 millions (for an aircraft weight of 75% of take-off weight) was also considered to evaluate the aerodynamic loads which are used to size the wing structure.

3.4. Methods, models and tools

3.4.1. Analysis and optimisation system

The optimisation system built and used for the winglet application is depicted in FIG 8. It is composed of two main components: the optimisation tool and an integrated

analysis system.

The optimisation tools (left hand-side of FIG 8), based on the DAKOTA optimisation toolkit [28] drives the optimisation process by conducting the design space exploration. DAKOTA embeds various numerical optimisation algorithms. The gradient optimiser CONMIN [29], implementing the method of feasible directions, has been used for the present optimisations.

The aero-structural analysis system, an evolution of already existing aerodynamic optimisation system [4], includes a parametric CFD mesh deformation module, the CFD code, the aerodynamic far-field analysis post-processor [27] and the wing structure weight evaluation modules. The integration of these different modules and the scheduling of the analysis makes use of Python scripts [30].

Along the optimisation process, the optimiser requests analysis for new winglet design by passing a design parameter vector to the analysis module. This design vector includes the value for the three parameters defining the winglet geometry and two additional aerodynamic variables corresponding to the angles of attack at the two investigated conditions. The analysis module proceeds by first generating a CFD mesh for the winglet geometry to be investigated using the mesh deformation module. CFD analyses for both the cruise condition and the manoeuvre conditions are then performed in parallel. From the results of the flow calculations at cruise condition, the aerodynamic drag and lift coefficient (CD_{cruise} and CL_{cruise}) are extracted with the far-field post-processor. The results of the flow calculation in manoeuvre condition is used to evaluate the lift coefficient and the spanwise aerodynamic wing loading. This aerodynamic wing loads are then used to evaluate the wing weight using a surrogate model build from a database of wing structure sizing for different winglet shape. Finally, these different analyses results, cruise drag, lift at both conditions and structural weight, are passed back to the optimiser which proceeds accordingly with the design space exploration.

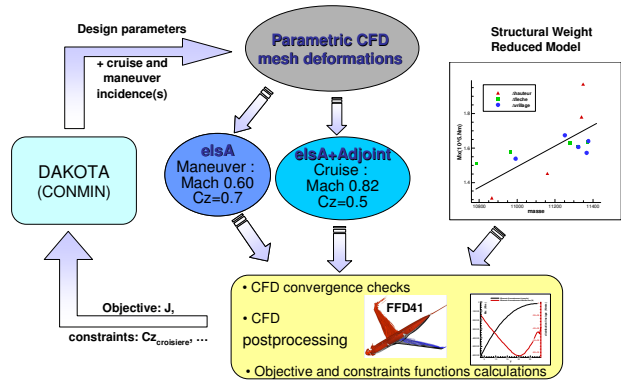


FIG 8. Optimisation system for aero-structural optimisation of a transport aircraft winglet

3.4.2. Aerodynamic modelling

All aerodynamic analyses performed in this work are based on Reynolds Averaged Navier-Stokes (RANS) calculations performed with the ONERA *elsA* [1] software, using the Spalart-Allmaras turbulence model. The coarse multi-block structured grids used during the optimisations

were composed of 2 blocks for about 400.000 cells (FIG 9). These different grids were produced with an in-house analytical (parametric) mesh deformation procedure applied to the baseline configuration grid (produced manually with the ANSYS-ICEM-Cfd mesh generator).

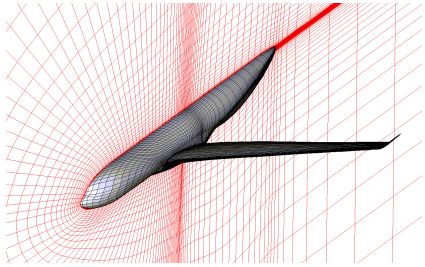


FIG 9. Aerodynamic model – Surface grid of the CFD mesh

3.4.3. Structural modelling

The structural modelling used in this study is based on MSC-NASTRAN Finite Element (FE) software. The structural model is presented in FIG 10. The main wing box and the winglet structure are included in this model and assumed to be composed of different aluminium alloys. The NASTRAN optimisation capability has been used to size the wing box structure by minimizing the structural weight of the wing with a constraint on the maximum allowed Von Mises stress of $\sigma_{VM}^{max} = 440$ MPa. The aerodynamic loads of a 2.5g manoeuvre have been used to stress the structure in this structural sizing process.

To evaluate the total wing structural weight $Weight_{wing}$, the winglet weight, which has been assumed to be proportional to its wetted surface (40 kg/m^2), was added to the wing box weight.

The total wing weight has been estimated with the previous procedure for a set of different winglet geometries sampling the intended design space. The different results were used to construct a surrogate model of the variation of the total wing weight with the winglet geometry and wing root bending moment.

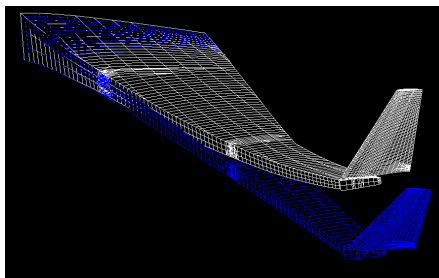


FIG 10. Wing Structure model – finite element model (FEM)

3.5. Results of the winglet optimisations

Two optimisations have been performed and are compared in this section. The first optimisation has been conducted with the aero-structural optimisation system as it is described in the previous section. The evolution of the design parameters and the objective and constraints functions during the optimisation are plotted in FIG 11.

The optimisation convergence is obtained in 14 gradient iterations for about 50 winglet design evaluations (about 100 CFD calculations), either for the gradients evaluations by finite difference or during the one-directional line search process of the CONMIN algorithm. The constraints on the lift coefficient in cruise and manoeuvre condition ($CL_{cruise} \geq 0.5$ and $CL_{manoeuvre} \geq 0.7$) are both satisfied at convergence, while the final design yields a reduction of the aero-structural objective function J of about 40 equivalent-drag counts (d.c.). This overall performance increase is obtained thanks to a reduction of the wing root bending moment of more than 1% which allows for a structural weight reduction, while the cruise drag is increased of about 1 d.c. The geometry of the optimised winglet is presented and compared to the baseline configuration in FIG 12. The aero-structurally optimised winglet design has a slightly reduced height and an increased sweep angle, the tip twist being only negligibly modified.

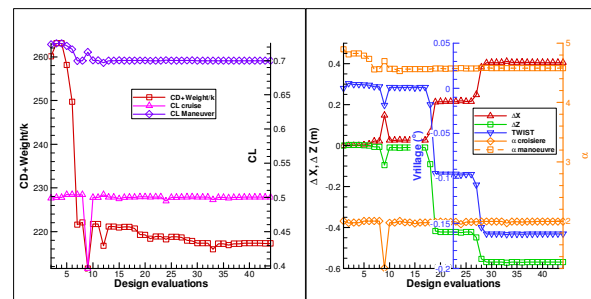


FIG 11. Convergence history of the aerodynamic-structure optimisation of the winglet

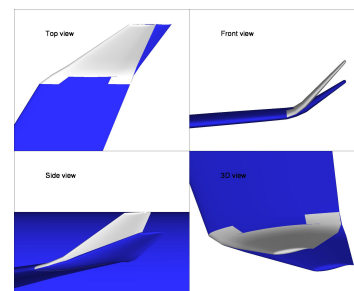


FIG 12. Comparison of the reference winglet geometry with the optimised design for aerodynamics performance only.

In order to evaluate the impact of accounting for the structural weight in the optimisation, a pure aerodynamic optimisation of the winglet has then been performed. For this pure aerodynamic optimisation, the analysis & optimisation system presented above has been slightly modified: the J function is here reduced to CD_{cruise} and the aerodynamic analysis in the manoeuvre condition has been switched off. The angle of attack for manoeuvre condition has also been removed from the design parameter vector and the corresponding constraint on the minimum lift in manoeuvre condition been deactivated. Finally, the gradient of cruise lift and drag were calculated here with the adjoint technique [7]. The optimisation history of this pure aerodynamic optimisation is presented in FIG 13. Convergence has been obtained within 9 iterations of the optimisation method which required 35 CFD calculations and 18 adjoint calculations. The

aerodynamically optimised winglet is compared to the baseline winglet in FIG 14. This optimal design differs from the baseline mainly by its height which has increased to the maximum value allowed to the optimiser. A 1.5 d.c. reduction of the cruise drag is achieved while maintaining the cruise lift above 0.5. An a posteriori analysis showed that the resulting wing bending moment at wing root is increased by 0.5%, which would require a significant wing structural reinforcement resulting in a weight increase not considered in this optimisation (the J function used for the previous MD optimisation increases by about 20 d.c.).

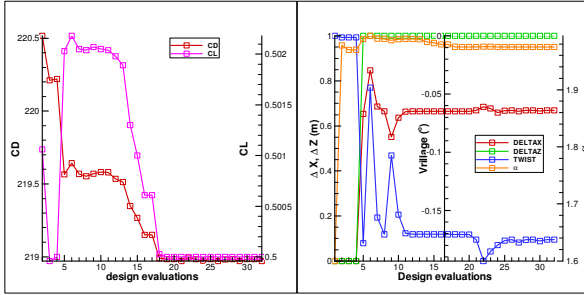


FIG 13. Convergence history of the pure aerodynamic optimisation of the winglet

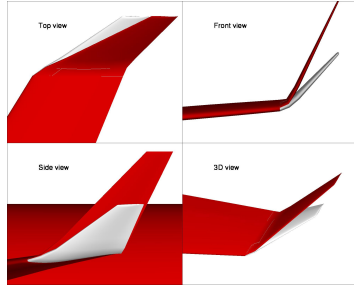


FIG 14. Comparison of the reference winglet geometry with the optimised design for aerodynamics performance only.

3.6. Concluding remarks

This work illustrates the possibility to evolve a single discipline (aerodynamic) optimisation system into a multi-disciplinary optimisation system where the additional disciplines are accounted for through reduced (surrogate) models constructed before the optimisation. This solution is suited for situations where the different disciplines are “weakly” coupled. In this work, an unidirectional coupling has been assumed: exchange from the aerodynamic to the structure through the manoeuvre loads used to size the wing structure and calculate its structural weight.

While keeping the assumption of rigid aerodynamic analysis, this approach could be improved through a direct coupling with the high fidelity structural analysis module, which has not been attempted in this work. If “stronger” coupling between the disciplines has to be considered, for instance to account for the aero-elastic deformations, more advanced approaches and techniques would be needed, as the one presented in the next section.

4. ADJOINT SENSITIVITY ANALYSIS OF STRONGLY COUPLED AERO-STRUCTURE SYSTEMS

α	Design parameters
D_α	Domain of design ($\alpha \in D_\alpha$)
J	Objective function
G_k	Constraint
r	Number of constraints
X	Fluid domain mesh
X_{rig}	Fluid domain mesh of the jig shape
Z	Structural domain mesh
R_α	Aerodynamic equations in residual form
W	Aerodynamic state variables
L	Aerodynamic Load
P	Pressure
S	Surface
R_s	Structural equations in residual form
F	Flexibility matrix
D	Structural displacements
ω	Bending displacement
θ	Twist displacement
λ_α	Aerodynamic adjoint vector
λ_s	Structural adjoint vector
C_x	Drag coefficient
C_z	Lift coefficient

TAB 1. Symbols used in multi-disciplinary linearised and adjoint equations

Weak coupling or sequential approaches perform well when disciplines are not too strongly coupled [10], e.g. when changes in one discipline do not significantly affect the other disciplines. It is then possible to ignore the effect of the variation of one discipline design parameters on the other disciplines during the optimization process of this discipline. By nature, the behaviour of an aircraft is multidisciplinary and depends on disciplines whose effects are deeply coupled. Aerodynamics and structures are among the most inter-twinned ones. For instance, if one attempts to maximize the lift produced by a wing while minimizing its drag and ignores the effects that the aerodynamic design variables have on the structural weight, he will necessarily hand up with an elliptic lift distribution. Structural optimization can still be performed holding the aerodynamic parameters fixed. The process might converge but nothing causes the result to be the true optimum of the coupled aero-structural system [33][38].

In order to find the optimum of a coupled system, the designer has no choice but taking the strong coupling effects into account. Several zero order methods can be employed such as grid searching, genetic algorithms, or simulated annealing for instance. Even though these techniques have the capacity of determining the optimum of functions with multiple local optima or discontinuities, they are not well suited for problems with a high number of parameters. In fact, in these cases, the number of function evaluations needed to locate the optimum rapidly becomes exorbitant. On the contrary, gradient-based methods are practically well adapted to optimization with a high number of parameters, but, depending on the initialization of the optimization algorithm, generally get trapped in the vicinity of a local optimum.

Aerodynamic shape optimization problems usually handle hundreds of variables. Since high-fidelity aerodynamic

analyses are particularly expensive, gradient-based methods are therefore extensively used [20][6][35][37]. The current session will then focus on the sensitivity analysis of aero-structural system.

The coupled system can be schematized as a set of black-boxes exchanging information through a possibly complex input/output network. The gradients needed by the optimization process depend on the sensitivities of the outputs with respect to the inputs. In the early beginning of aerodynamic shape optimization, these sensitivities were computed by finite differentiation. Since this technique being time-consuming and inaccurate is now a well-known fact, it has rather quickly been replaced by analytical methods. The vector composed of the sensitivities of the outputs with respect to the inputs is then solution of the global sensitivity equations GSE [36] related to the coupled system. For a coupled system this technique is referred to as the coupled direct method. Recently, the use of the adjoint method has significantly reduced the number of systems to solve when the number of design parameters is greater than the number of functions to differentiate during the optimization process. Focusing only on aeroelastic systems, these techniques have been applied to simple linear models first, and then to nonlinear cases, using the direct method [32] and the adjoint method later [9] [34].

An adjoint sensitivity analysis framework is currently under development at ONERA. It aims at computing the sensitivities required by the aerodynamic shape optimization process of an aeroelastic system, namely the gradient of the objective function and of the constraints with respect to the design parameters. Assuming that we have translated the optimization problem into a minimization problem, and that we have transformed every constraint to be an inferiority constraint, the optimization problem is:

find $\alpha \in D_\alpha$ such that J is minimum and $G_k < 0, 1 \leq k \leq r$.

Currently, the aerodynamic behaviour is captured by the Euler equations, and structural displacements are described by beam theory. This assumption enables the designer to have a fairly good approximation of the displacements of high aspect ratio wings. So that, only the wings of the studied configuration will be assumed to have a flexible motion while the fuselage will remain at a fixed position. The influence coefficients matrix or flexibility matrix approach [31] is used to predict structural displacements. The aeroelastic system of equations is given by Equation (1).

$$(1) \quad \begin{cases} R_a(W, X) = 0 \\ R_s = D - FL = 0 \end{cases}$$

Since the fluid mesh X and the aerodynamic loads respectively depend on the structural displacements D and the fluid state variables W (Equation (2)), the above system is strongly coupled as described by FIG 15.

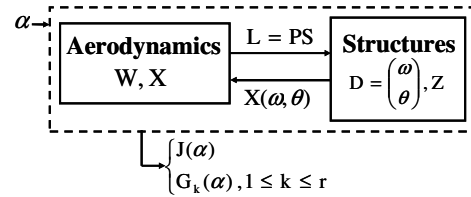


FIG 15. Aeroelastic system interactions scheme.

$$(2) \quad \begin{cases} X(X_{rig}, Z, D) \\ L(X, Z, W) \end{cases}$$

The static aeroelastic equilibrium is predicted according to a fixed point algorithm. Since we will only study configurations with small structural displacements amplitude, the small displacement hypothesis is taken. The structural mesh Z remains fixed during the fixed point iterations. The aerodynamic loads on the structure, only due to pressure forces in our case, are transferred to the structural mesh through a consistent and conservative process.

The coupled direct system of equations is deduced from the differentiation of the system of equations (1). The coupled adjoint system of equations is deduced from the coupled direct system and from the gradient of the function one wishes to evaluate (Equation (3)).

$$(3) \quad \frac{dJ}{d\alpha} = \frac{\partial J}{\partial \alpha} + \frac{\partial J}{\partial W} \frac{dW}{d\alpha} + \frac{\partial J}{\partial D} \frac{dD}{d\alpha} + \frac{\partial J}{\partial X} \frac{dX}{d\alpha} + \frac{\partial J}{\partial Z} \frac{dZ}{d\alpha}$$

These two systems are solved using a lagged iterative technique respectively described by Equations (4) and (5), n being the current iteration index.

$$(4) \quad \begin{cases} \frac{\partial R_a}{\partial W} \left(\frac{dW}{d\alpha} \right)^n = - \frac{\partial R_a}{\partial X} \left(\frac{\partial X}{\partial X_{rig}} \frac{dX_{rig}}{d\alpha} + \frac{\partial X}{\partial Z} \frac{dZ}{d\alpha} + \frac{\partial X}{\partial D} \left(\frac{dD}{d\alpha} \right)^n \right) \\ \left(\frac{dD}{d\alpha} \right)^n = F \left(\frac{\partial L}{\partial W} \left(\frac{dW}{d\alpha} \right)^n + \frac{\partial L}{\partial X} \left(\frac{\partial X}{\partial X_{rig}} \frac{dX_{rig}}{d\alpha} + \frac{\partial X}{\partial Z} \frac{dZ}{d\alpha} + \frac{\partial X}{\partial D} \left(\frac{dD}{d\alpha} \right)^{n-1} \right) \right) \\ \quad + \frac{\partial L}{\partial Z} \frac{dZ}{d\alpha} \end{cases}$$

$$(5) \quad \begin{cases} \left(\frac{\partial R_a}{\partial W} \right)^T (\lambda_a)^n = - \left(\frac{\partial J}{\partial W} \right)^T + \left(F \frac{\partial L}{\partial W} \right)^T (\lambda_s)^n \\ (\lambda_s)^n = - \left(\frac{\partial J}{\partial X} \frac{\partial X}{\partial D} \right)^T - \left(\frac{\partial R_a}{\partial X} \frac{\partial X}{\partial D} \right)^T (\lambda_a)^{n-1} + \left(F \frac{\partial L}{\partial X} \frac{\partial X}{\partial D} \right)^T (\lambda_s)^{n-1} \end{cases}$$

These two methods have been validated on the DLR F4 wing-fuselage configuration placed in a transonic flow at Mach 0.75, and 0.93-degree angle of attack. The beam characteristics are summarized in TAB 2.

Young's modulus	$E = 1.813 \cdot 10^{11} \text{ N/m}^2$
Shear modulus	$G = 0.682 \cdot 10^{11} \text{ N/m}^2$
Poisson's ratio	$\nu = 0.33$
Beam mesh size	250 points

TAB 2. Beam characteristics

The sensitivity of the aerodynamic coefficients with respect to a change in the built-in twist of the wing are illustrated in TAB 3, and TAB 4 shows their sensitivities to a span wise bumping on the wing. These coefficients

have been computed using ffd41 [26][27].

	Direct Equations	Adjoint Equations	Finite Differences
$dC_x/d\alpha$	-0.0031450	-0.0031447	-0.0031375
$dC_z/d\alpha$	-0.03965	-0.03966	-0.03965

TAB 3. Aerodynamic coefficients sensitivity with respect to built-in twist.

	Direct Equations	Adjoint Equations	Finite Differences
$dC_x/d\alpha$	0.0318362	0.0318405	0.0318483
$dC_z/d\alpha$	0.3580606	0.3580715	0.3590000

TAB 4. Aerodynamic coefficients sensitivity with respect to spanwise bumping.

The results obtained in these first coupled sensitivities calculations with both linearised and adjoint methods and using an inviscid flow model and a beam structure model have been validated against finite difference. This work is currently ongoing with the objective to extend these methods to be applicable to viscous turbulent flow and higher fidelity model of the structure.

5. CONCLUSION

This paper illustrates different approaches to extend an aerodynamic design optimisation process towards a multi-disciplinary (aerodynamic and structure) optimisation process. Through the application of multi-disciplinary design optimisation to two different aircraft components, an engine pylon and a winglet, an approach using reduced models to take into account the influence of the structure in the optimisation process are illustrated. This approach is applicable to multi-disciplinary system presenting weakly coupled (or uncoupled) disciplines. For systems presenting a stronger coupling between disciplines, an approach based on the extension of the aerodynamic adjoint method to multi-disciplinary systems, currently under development, is presented. This paper illustrates different pragmatic solutions intended to progress towards high-fidelity multi-disciplinary optimisation.

ACKNOWLEDGEMENTS

The authors would like to thank the French government DPAC and UMAERO agencies and the European Commission for funding this research work within the French DTP-OPTIMISATION program and the VIVACE integrated EU project. The fruitful collaboration with AIRBUS is also acknowledged.

REFERENCES

- [1] L. Cambier, M. Gazaix, *e/sA: An Efficient Object-Oriented Solution to CFD Complexity*, AIAA 2002-0108, Reno, January 14-17, 2002.
- [2] Samareh, J.A., Survey of Shape Parameterization Techniques for High-Fidelity Multidisciplinary Shape Optimization, AIAA JOURNAL Vol. 39, No. 5, May 2001.
- [3] Brenda M. Kulfan and John E. Bussoletti., "Fundamental" Parametric Geometry Representations for Aircraft Component Shapes, AIAA Paper 2006-6948 11th AIAA/ISSMO Multidisciplinary Analysis and Optimization Conference, 6 - 8 September 2006.
- [4] M. Meaux, M. Cormery, Viscous Aerodynamic Shape Optimization Based on the Discrete Adjoint State for 3D Industrial Configurations, ECCOMAS 2004, Jyväskylä, Finland, July 24-28, 2004.
- [5] O. Pironneau, *Optimal Shape Design for Elliptic Systems*, Springer-Verlag, New-York, 1984.
- [6] A. Jameson, Aerodynamic Design Via Control Theory, Journal of Scientific Computing, Vol 3., p 233-260, 1988.
- [7] J. Peter, Discrete Adjoint Techniques in *e/sA* (part 1): Method/Theory, ONERA-DLR Aerospace Symposium, Toulouse, October 4-6, 2006.
- [8] G. Carrier, Single and Multi-point Aerodynamic Optimizations of a Supersonic Transport Aircraft Wing using Optimization Strategies Involving Adjoint Method and Genetic Algorithm, ERCOFTAC, Las Palmas, April 5-7, 2006.
- [9] G. Carrier, I. Salah el Din, S. Mouton, Discrete Adjoint Techniques in *e/sA* (part 2): Application to Aerodynamic Design Optimisation, ONERA-DLR Aerospace Symposium, Toulouse, October 4-6, 2006.
- [10] G. Carrier, Multi-Disciplinary Optimization of a Supersonic Transport Aircraft Wing Planform, ECCOMAS 2004, European Congress on Computational Methods in Applied Sciences and Engineering, Jyväskylä, Jul. 2004.
- [11] J.P. Bècle, P. Mogilka, Powerplant Integration for Transport Aircraft at Cruise Conditions, French experience, International Forum on Turbine Powered Simulations, DNW Emmeloord, May 16-17, 1995.
- [12] A. Garcia, Intégration des systèmes propulsifs, choix et compromis, colloque AAAF Aéropropulsion 1990, Paris, March 20-21, 1990.
- [13] D.R. Jones, M. Schlonlau, W.J. Welch, Efficient Global Optimisation of Expensive Black-Box Functions, Journal of Global Optimisation, Vol. 13, pp. 455-492, 1998.
- [14] K.C. Hackett, P.H. Rees, J.K. Chu, Aerodynamic Design Optimisation Applied to Civil Transports with Underwing Mounted Engines, 21st ICAS congress, Melbourne, September 13-18, 1998.
- [15] D.A. Naik, A.M. Ingraldi, O.C. Pendergraft, Experimental Study of Pylon Geometries for Transport Aircraft, AIAA-92-0153, Reno, January 6-9, 1992.
- [16] D.A. Naik, Innovative Pylon Concept for Engine-Airframe Integration for Transonic Transport, AIAA-89-1819, 1989.
- [17] D. Destarac, J. Reneaux, Applications de l'optimisation numérique à l'aérodynamique des avions de transport, La Recherche Aérospatiale, No. 2, 1993
- [18] J.L. Godard, O.-P. Jacquotte, Analyse détaillée de

- l'interaction voilure-nacelle d'un avion de transport civil, AGARD CP-498, 1992.
- [19] J.L. Godard, H. Hoheisel, C.C. Rossow, V. Schmitt, Investigation of Interference Effects for Different Engine Position on a Transport Aircraft Configuration, Workshop on Aspects of Airframe Engine Integration for Transport Aircraft, Braunschweig, March 6-7, 1996.
- [20] R.M. Hicks, P.A. Henne, Wing Design by Numerical Optimisation, *Journal of Aircraft*, Vol. 15, pp. 407-412, 1978.
- [21] S. Viala, S. Amant, L. Tourette, Recent Achievements on Navier-Stokes Methods for Engine Integration, CEAS Aerospace Aerodynamics Research Conference, paper 54, Cambridge, June 10-13, 2002.
- [22] J. Peter, C.-T. Pham, F. Drullion, Contribution to Discrete Implicit Gradient and Discrete Adjoint Method for Aerodynamic Shape Optimisation, Jyvaskyla, Finland, ECCOMAS 2004, July 24-28, 2004.
- [23] B. Chandrasekaran, Computation and Comparison of the Installation Effects of Compression Pylons for a High Wing Transport, AIAA-88-0004, Reno, January 11-14, 1988.
- [24] A.W. Chen, E.N. Tinoco, PAN AIR Applications to Aero-Propulsion Integration, *Journal of Aircraft*, Vol. 21, No. 3, pp. 161-167 1984.
- [25] S. Mouton, J. Laurenceau, G. Carrier, Aerodynamic and Structural Optimisation of Powerplant Integration under the Wing of a Transonic Transport Aircraft, 42^{ème} Colloque d'Aérodynamique Appliquée AAAF, Sophia-Antipolis, March 19-21, 2007
- [26] J. van der Vooren, D. Destarac, Drag / Thrust Analysis of Jet-Propelled Transonic Transport Aircraft: Definition of Physical Drag Components, *Aerospace Science and Technology*, Vol. 8, No. 7, October 2004.
- [27] D. Destarac, Far-Field/Near-Field Drag Balance and Applications of Drag Extraction in CFD, VKI Lecture Series 2003, CFD-Based Aircraft Drag Prediction and Reduction, National Institute of Aerospace, Hampton (VA), Nov. 2003.
- [28] <http://endo.sandia.gov/DAKOTA/software.html>
- [29] G.N. Vanderplaats, CONMIN – A Fortran Program for Constrained Function Minimization – User's Manual, NASA TM X 62.282, August 1973.
- [30] G. van Rossum, *Python Reference Manual*. Centrum voor Wiskunde en Informatica (CWI), Report number CS-R9525, 1995.
- [31] R. Bisplinghoff, H. Ashley and R. Halfman, *Aeroelasticity*, Dover Science Book, 1996.
- [32] A. Giunta, A Novel Sensitivity Analysis Method for High-Fidelity Multidisciplinary Optimization of Aero-Structural Systems, AIAA Paper 2000-16542.
- [33] J. Martins, A Coupled-Adjoint Method for High-Fidelity Aero-Structural Optimization, PhD Thesis, Stanford University, Nov. 2002.
- [34] K. Maute, M. Nikbay and C. Farhat, Sensitivity Analysis and Design Optimization of Three-Dimensional Nonlinear Aeroelastic Systems by the Adjoint Method, *International Journal for Numerical Methods in Engineering*, Vol. 56, 2003.
- [35] O. Pironneau, On Optimal Shapes for Stokes Flow, *Journal of Fluid Mechanics*, Vol.70, No.2, 1973.
- [36] J. Sobieszcsanski-Sobieski, Sensitivity of Complex, Internally Coupled Systems, *AIAA Journal*, Vol.28, No.1, 1990.
- [37] G. Vanderplaats and R. Hicks, Numerical Airfoil Optimization Using a Reduced Number of Design Coordinates, Technical Report TMX 73151, NASA, 1976.
- [38] S. Wakayama, Lifting Surface Design Using Multidisciplinary Optimization, PhD Thesis, Stanford University, Dec. 1994.